Tamap Journal of Engineering
http://www.tamap.org/

doi:10.29371/2019.3.78
Volume 2019, Article ID 78
Research Article

Inclination Angle Influence on Cavitating Marine Propeller

Sakir BAL

Naval Architecture and Marine Engineering Department, Istanbul Technical University, 34469 Istanbul, Turkey
E-mail: sbal@itu.edu.tr

Received: 18.09.2019 • **Accepted**: 28.10.2019 • **Published Online:** 30.10.2019

Abstract: In this study, the effects of inclination shaft angle on the hydrodynamic performance of cavitating marine propellers are investigated by a numerical method developed before. The cavitaitng blades are represented by source and vortex elements. The cavity characteristics such as; cavitation form, cavity volume, cavity length etc. of blades are computed at a given cavitation number and a fixed advance coefficient. A lifting surface method is applied for these calculations. Numerical lifting surface method is validated with experimental results of DTMB 4119 model benchmark propeller. The effects of inclination shaft angle on thrust, torque coefficients and efficiency values of the propeller are examined by a parametric study. By changing the inclination angles of propeller, the thrust, torque and efficiency are computed and compared with each other. The influence of inclination shaft angle on cavity patterns on the blades are also discussed.

Keywords*:* marine propeller, cavitation, inclination angle, lifting surface method

1. INTRODUCTION

Small or medium-sized naval vessels can utilize propellers on inclined shafts. The forces, torques and even cavity patterns generated by inclined shaft propellers are different than those of conventional (non-inclined) shafts. This difference can be larger with an increase in angle of inclined shaft. Therefore, the influence of inclined shaft on hydrodynamic performance of cavitating propellers is significant and should be investigated in the design process of propellers.

It is well-known that flow around a marine propeller with an inclined shaft is unsteady even under open water conditions. In the past, an unsteady propeller analysis and design method was developed in [1, 2]. An axisymmetric RANS (Reynolds Averaged Navier-Stokes) calculation and the vortex lattice design method was coupled in [3]. In the method, while the effective wake input for the vortex lattice design method was provided by RANS computation, the propeller force is transfered as the body force to the RANS domain. Griffin and Kinnas further improved the propeller analysis and design methods [4]. In particular, the analysis method was improved in a such way that the cavity search algorithm was included along the blade section. The design method was also extended to include the skew distribution and minimum pressure constraint. In another study, an unsteady analysis method was extended to apply for the podded propellers succesfully [5]. An iterative technique was developed by seperating the pod part, the strut part and the part of propeller blades. The results of the method converged very fast and it was also suggested for other multi-component propulsor systems. Two different numerical approaches, namely RANS solver and a panel method were addressed and applied for the analysis of unsteady flow around marine propellers subjected in an oblique inflow in [6]. Cavitation on the other hand was not considered in the study. RANS solvers were also applied for the analysis of steady and unsteady propeller performances in [7]. The effects of wake modelling on propeller cavitation have been investigated experimentally under inclined shaft condition in [8]. The accurate prediction of the steady and unsteady propulsor forces and torques arising from operation of propulsor in non-uniform wakes was also modelled numerically in the preliminary design or later stages of analysis of any propulsor in [9]. However, no cavitation was included into the calculations. A systematic study of comparison between RANS solver and a panel method for propeller analysis was presented in [10]. The effects of cavitation on propeller performance was not considered in this study. But reliability of panel method was discussed in a detailed manner. A very recent overview of the hydrodynamic aspects of marine propellers under unsteady flow conditions was published in the book of [11].

In the past, a search algorithm for cavity detachment for back and mid-chord cavitation was also added in the lifting surface method [12, 13]. The viscous effects were assumed to be dominant near the leading edge of the blade

sections. Later, a numerical method based on [12] was developed in [14]. This method improved significantly the cavitation simulation on the blades of the propeller [14]. A simpler method based on a lifting line model to compute the propeller hydrodynamic performance was also later introduced in [15]. Cavitation has been modelled by RANS and DES (Detached Eddy Simulation) under inclined shaft condition in [16]. It has been reported that this technique has improved the simulation results significantly. The wake alignment procedure that is very important for inclined shaft propeller has been investigated in [17]. Panel method was applied for hydrodynamic analysis of cavitating propeller. In this study, the characteristics of unsteady flow around cavitating propeller and propeller performance have been investigated by a lifting surface method. The propeller shaft inclination is especially emphasized here. The cavitaitng blades of the propeller can be represented by source and vorticity elements [12]. The blade loading and vorticity in the trailing wake can also be represented by vortex lattices distributed on the mean camber surface while the blade thickness can be accounted for by adding thickness source panels. The strength of singularities of vortex/source distributions are unknown. The strengths can then be found by applying the appropriate boundary conditions on the blades [18, 19]. The steady loading as well as the unsteady forces and cavitation characteristics on the blades can also be predicted by this lifting surface method. This method is applied to DTMB 4119 model propeller and the effects of inclination shaft angle on the results are discussed.

2. NUMERICAL METHOD

A lifting surface method developed before is applied to calculate the propulsive performance of a marine propeller as similar to the one given in [19]. This method is summarized here for the completeness of the paper. The flow around propeller is assumed to be incompressible, inviscid and irrotational. Total velocity q around propeller can be given as follows:

$$\vec{q}(x,y,z,t) = \vec{U}(x,y,z,t) + \nabla\phi(x,y,z,t) \tag{1}$$

Here ϕ is the perturbation potential due to propeller and U is the velocity of incoming uniform flow. Perturbation potential should satisfy Laplace equation in the region,

$$\nabla^2\phi = 0 \tag{2}$$

The propeller blades, including wakes are discretized into elements of vortices and sources (Figure 1). The singularities are distributed on the camber lines of the propeller blade sections. This method is thus classified as a lifting surface method since the singularities (vortices and sources) are distributed on the mean camber surface. The strengths of singularities can be found by applying kinematic body condition,

$$\frac{\partial\phi}{\partial n} = -\vec{U}.\vec{n} \tag{3}$$

Here, n is unit normal vector on the selected control points on the blades.

The vortices distributed over the blades are divided into two parts; bound and trailing vortices. The bound vortices, located in the radial direction, are to simulate the load distribution on the propeller blade. The trailing vortices are located in the direction of the flow, obtained from the different intensities of adjacent bound vortex elements. A number of source elements are taken at adjacent bound vortex to simulate the thickness of the blade. The strengths of vortex are calculated by solving a set of simultaneous equations which satisfy the flow tangency (kinematic boundary) condition at the blade control points. The discretized form of the kinematic boundary condition can be written as:

$$\sum_{\Gamma}\Gamma\,\vec{v}_{\Gamma}\cdot\vec{n}_m = -\vec{v}_{in}\cdot\vec{n}_m - \sum_{Q_B}Q_B\,\vec{v}_Q\cdot\vec{n}_m - \sum_{Q_C}Q_C\,\vec{v}_Q\cdot\vec{n}_m \tag{4}$$

where $\vec{v}_{\Gamma}$ is the velocity vector induced by each unit strength vortex element, $\vec{v}_Q$ is the velocity vector induced by each unit strength source element, $\vec{n}_m$ is the unit vector normal to the mean camber line or trailing wake surface. The induced velocities due to vortex elements of the lifting surface are calculated using Biot-Savart's law expressed as:

$$\vec{V}_{\Gamma} = \frac{\Gamma}{4\pi}.\frac{\vec{L}x\vec{d}}{\vec{d}^3} \tag{5}$$

where $\vec{V}_\Gamma$: induced velocity, Γ: circulation, $\vec{L}$: vortex length element, $\vec{d}$: distance between the element and the field point. The induced velocities due to sources/sinks are also computed on the basis of given source/sink intensity.

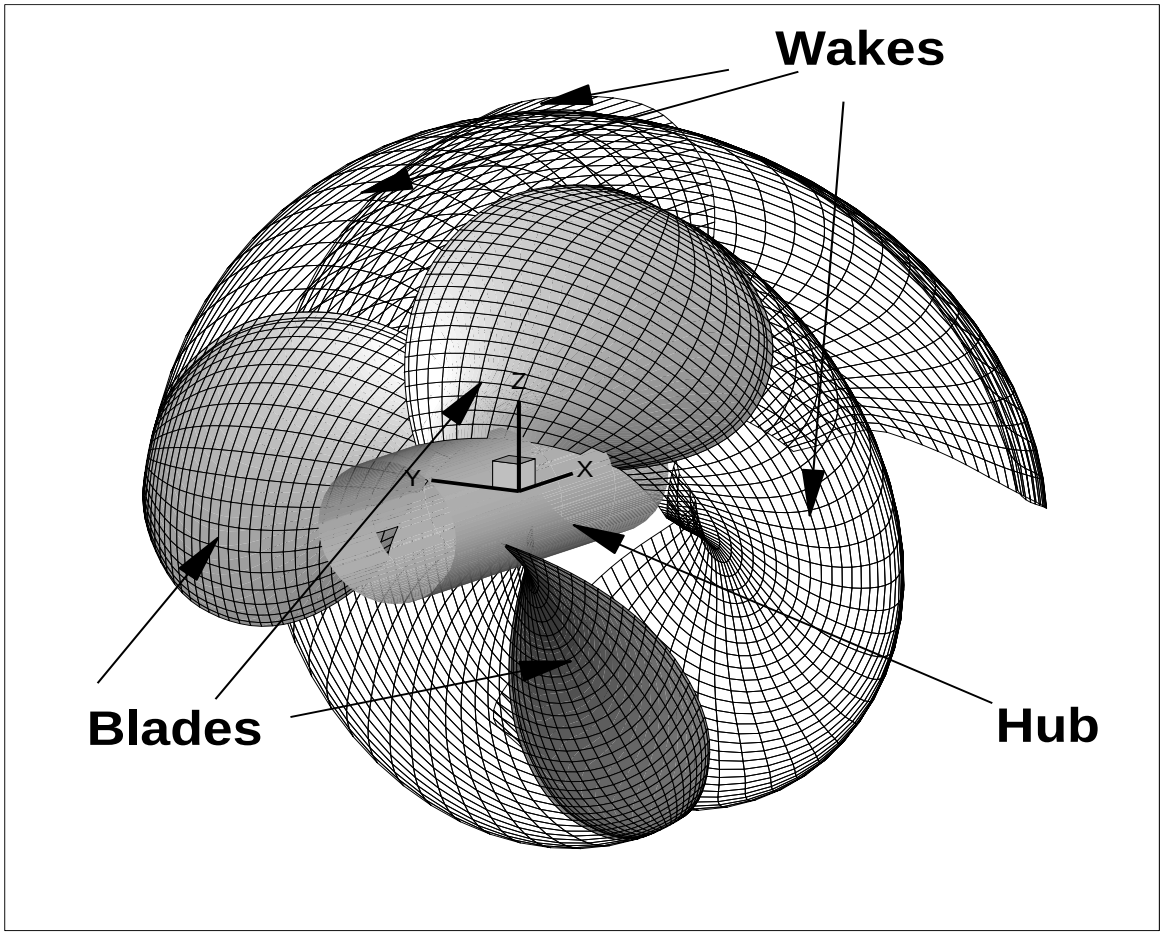

Figure 1. Panels on blades, wakes of propeller and the definition of coordinate system.

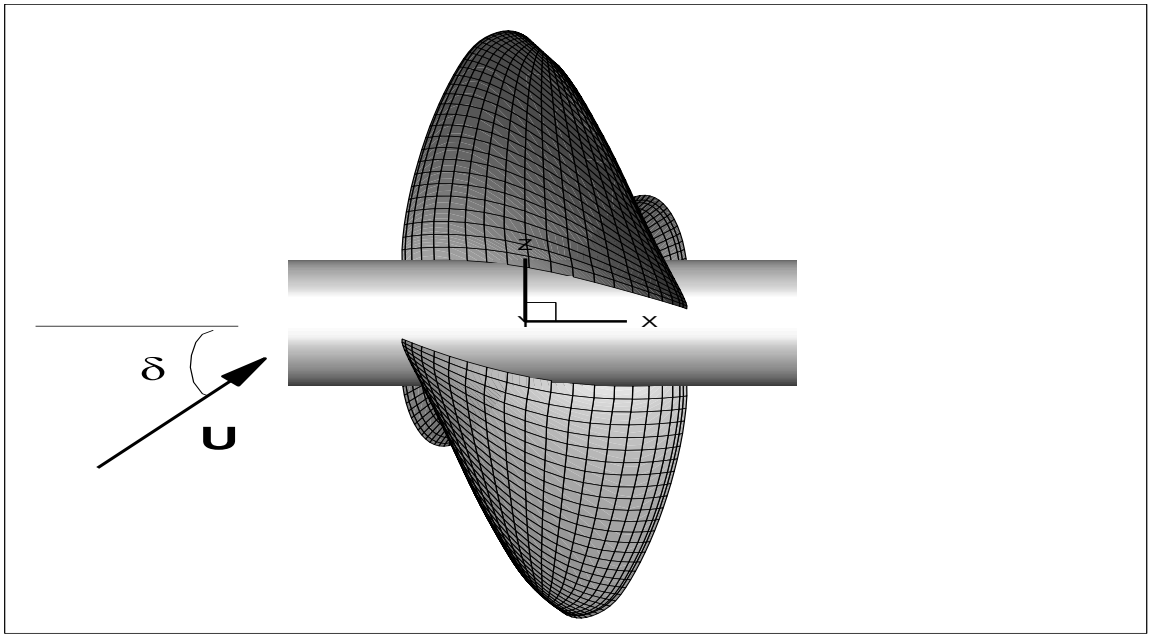

Figure 2. Definition of shaft inclination angle.

In the lifting surface method, the formation and decay of the cavity can also occur instantaneously depending only on whether the pressure exceeds the vapor pressure. It is assumed that the cavity starts at the leading edge of the blade and vanishes at the cavity trailing edge. Cavity thickness varies linearly along each cavity panel in the chord-wise direction. It is assumed that the viscous force is computed based on the frictional drag coefficient, C_f, which is applied uniformly on the wetted surfaces of blades. Once the bound vortex elements intensity is obtained, then the velocity induced by the propeller in any point in space can be computed by using five angular position of the propeller blade. Finally, the arithmetic average of these five values becomes the induced velocity at the corresponding point. The forces on the propeller blade are found by adopting the law of Kutta-Joukowsky. If the propeller is working in a steady state condition, the forces on all blades are same. Hence, the force on the entire propeller is found by multiplying each blade force by the number of blades. Hub effect using the method of images can also be included into the calculations. The inclination angle (δ) of propeller shaft is also shown in Figure 2. Refer to [19] for details of the lifting surface method of solution applied to the propeller analysis problem.

3. RESULTS and DISCUSSION

First, the lifting surface method is applied for validation to non-cavitating DTMB 4119 model propeller [19, 20]. The propeller inflow is uniform and there is no inclined shaft ($\delta = 0^o$). The propeller has three blades, NB = 3. The DTMB 4119 propeller has also the following geometric dimensions and operational conditions:

- The hub to diameter ratio is 0.2.
- The blade geometries from reference [19] in terms of radial distribution of the chord length (c), camber (f), thickness (t) and pitch (P) are shown in Table 1.
- The blade sections are designed with using NACA 66 modified profiles and a = 0.8 camber line [19].
- The original propeller has no skew and no rake.

The number of vortex elements is (N=20) in the chord-wise direction and (M=30) in the radius direction of blades. These number of panels have been found to obtain converged results after some numerical tests. The frictional drag coefficient was assumed to be C_f=0.0035 in the calculations. The front side view of DTMB 4119 model propeller and the panels used on the blades are shown in Figure 3. The thrust and torque coefficients (K_T and K_Q) and efficiency ($\eta = \frac{J}{2\pi}\frac{K_T}{K_Q}$) of the propeller versus advance coefficients (J) computed from the analysis are compared with experiments as shown in Figure 4. The agreement between the results of analysis method and experiments is satisfactory.

Table 1. DTMB 4119 propeller geometry from [19].

r/R	**c/D**	**P/D**	**t_{max}/c**	**f_{max}/c**
0.20	0.3200	1.1050	0.2055	0.0143
0.30	0.3635	1.1022	0.1553	0.0232
0.40	0.4048	1.0983	0.1180	0.0230
0.50	0.4392	1.0932	0.0902	0.0218
0.60	0.4610	1.0879	0.0696	0.0207
0.70	0.4622	1.0839	0.0542	0.0200
0.80	0.4347	1.0811	0.0421	0.0197
0.90	0.3613	1.0785	0.0332	0.0182
0.95	0.2775	1.0770	0.0323	0.0163
0.98	0.2045	1.0761	0.0321	0.0145
1.00	0.0800	1.0750	0.0316	0.0118

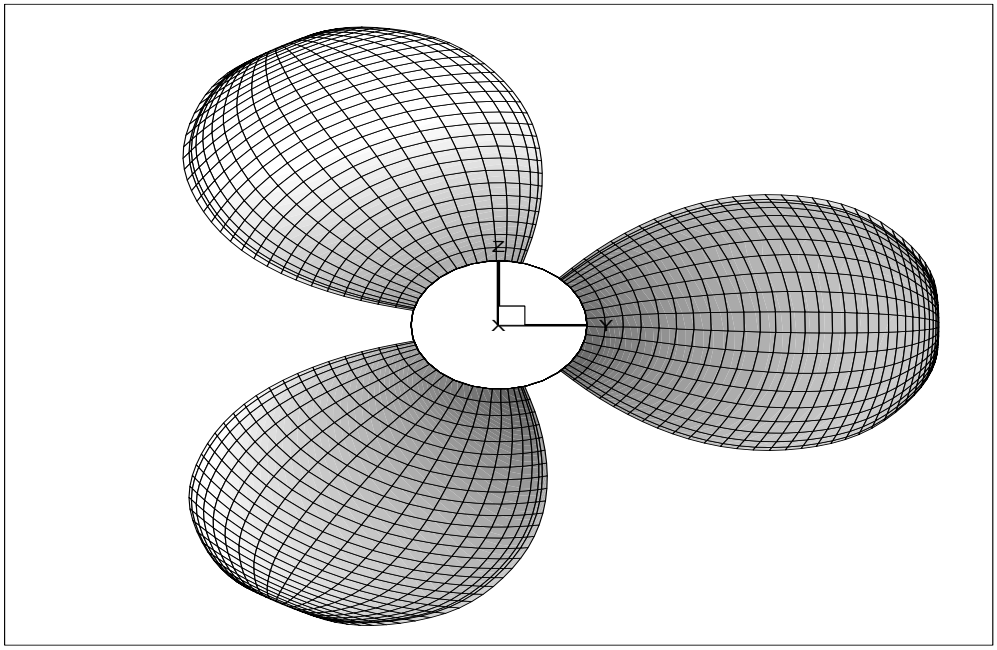

Figure 3. Geometry and panels used on DTMB 4119 propeller.

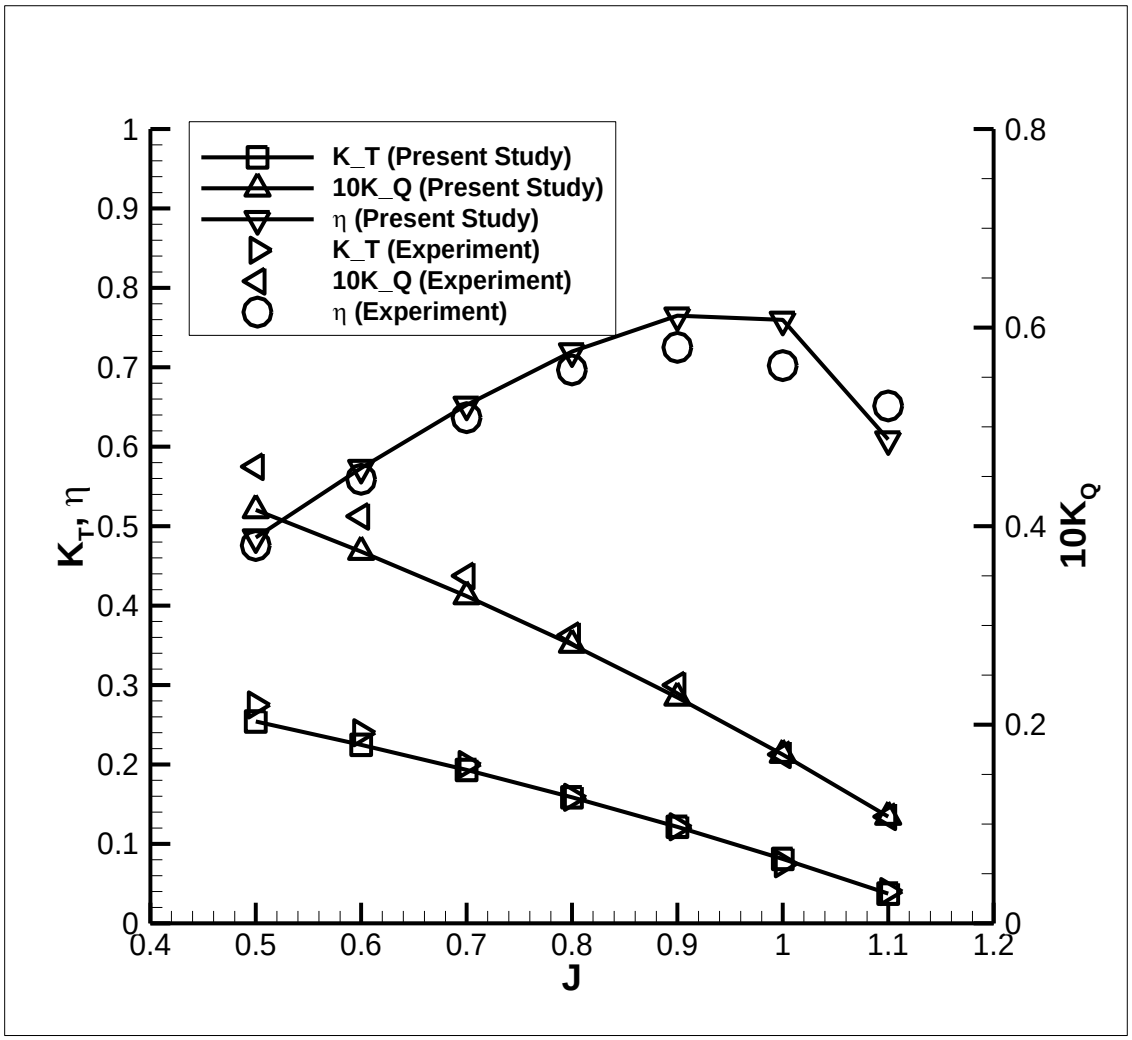

Figure 4. Comparison of K_T, K_Q and η values with experiments (DTMB 4119).

Later, the method is applied to cavitating DTMB 4119 model propeller. Advance coefficient is J = 0.8 and the cavitation number is selected as σ = 1.2. The cavitation number is defined as,

$$\sigma = \frac{p - p_v}{0.5\rho(nD)^2} \tag{6}$$

Here, p is the static pressure on the shaft of propeller, p_v is the vaporize pressure. The computed cavitation patterns on blades for different shaft inclination angles ($\delta = 0^o$, 5^o and 10^o) are shown in Figures 5, 6 and 7, respectively. As you can see from these figures that, an increase in inclination angle causes a decrease in cavitation volume on the blade of the top (upper) side while an increase on the blade of the bottom (lower) side. This is an expecting phenomenon since the blade of the bottom side meets the flow first under inclined shaft conditions. On the other hand, increasing inclination angle causes a decreasing thrust and torque coefficients while there is almost no change in efficiency values as shown in Table 2. Note also that in Figure 5, all cavity formations on blades are same since the incoming flow is uniform and the inclination angle for this case is equal to zero. In Figure 8, the average loading (circulation) distribution versus inclination angle of propeller shaft is shown. It is clear that the loading particularly near the root region is decreasing with an increase in inclination shaft angle. This confirms the results given in Table 2. On the other hand, there is no change on loading near tip region with an increase in inclined shaft angle.

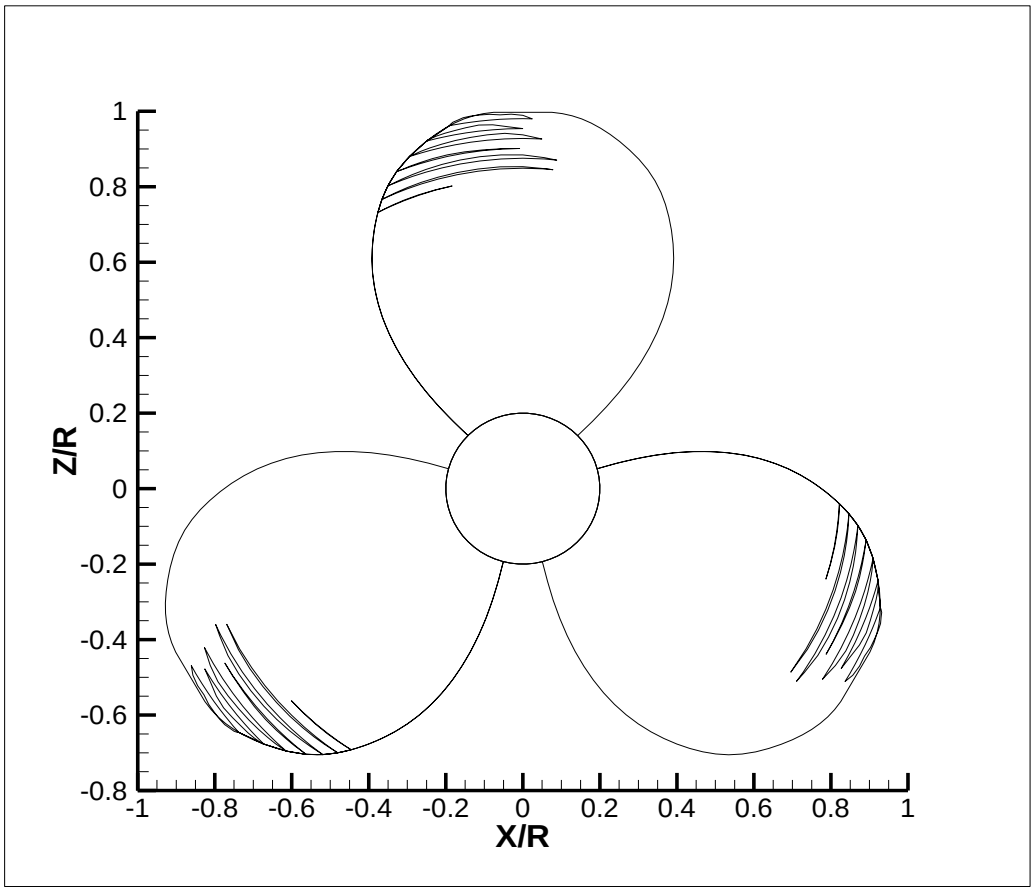

Figure 5. Cavitation pattern on blades for J=0.8, σ=1.2 and δ=0º.

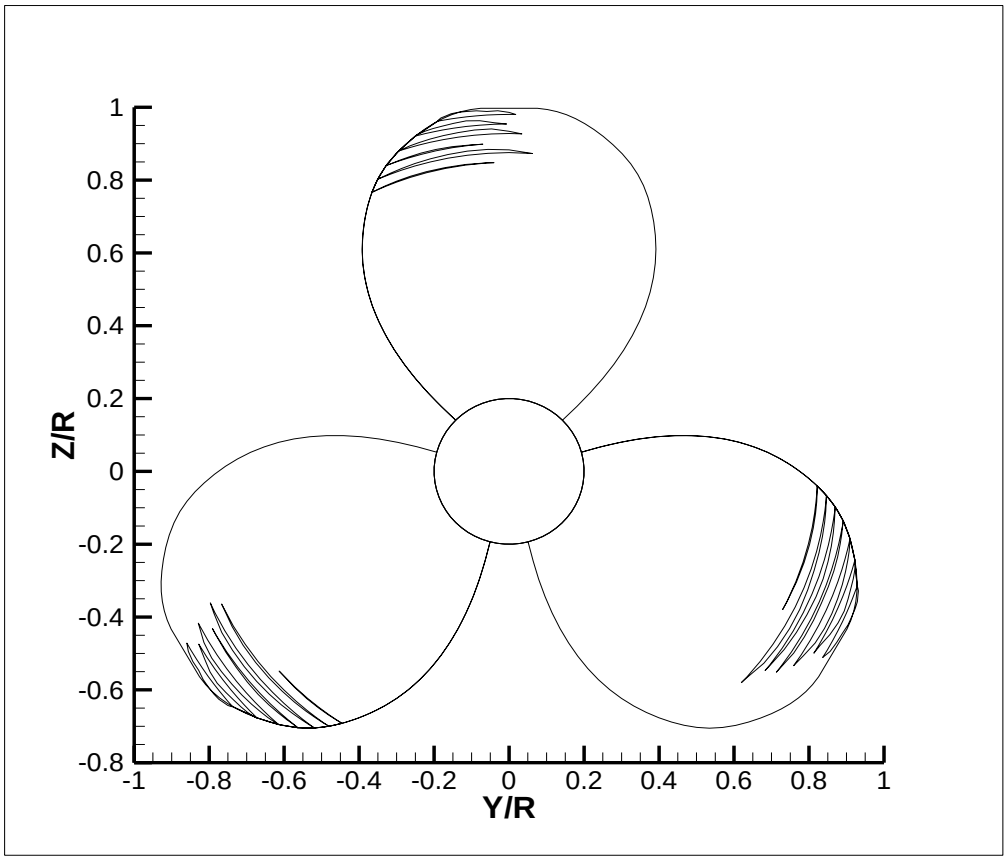

Figure 6. Cavitation pattern on blades for J=0.8, σ=1.2 and δ=5º.

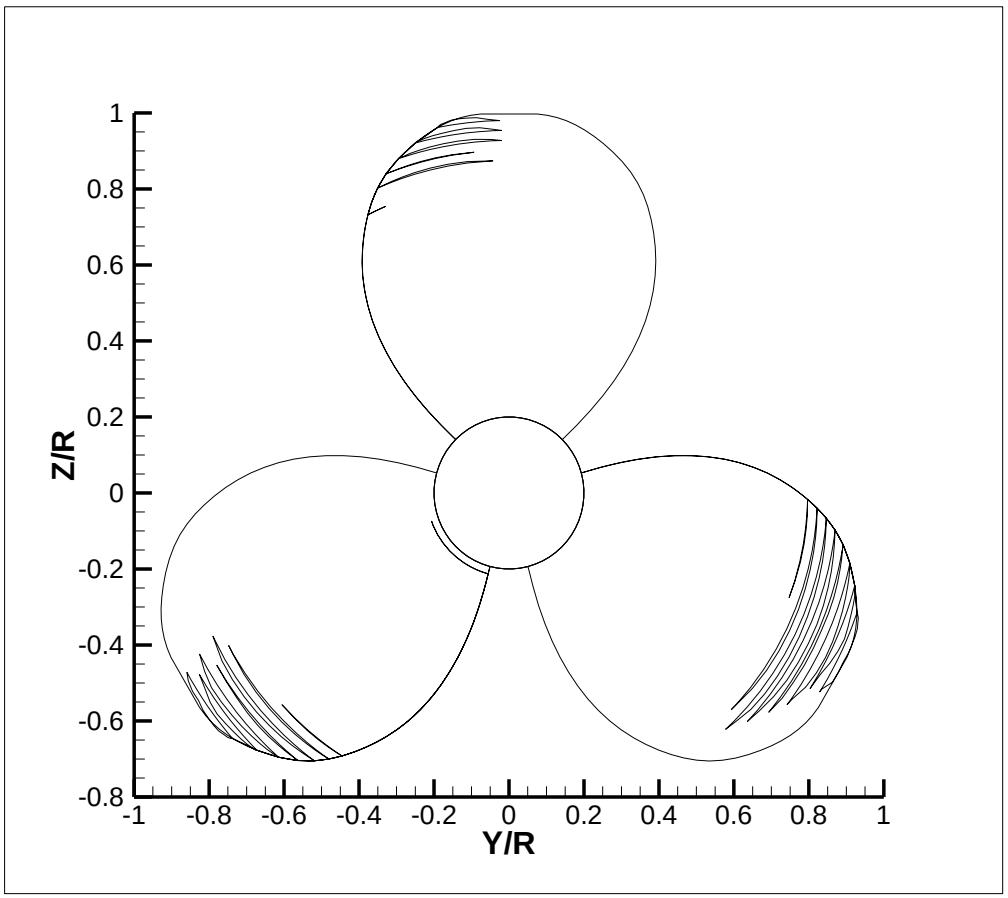

Figure 7. Cavitation pattern on blades for J=0.8, σ=1.2 and δ=10º.

Table 2. Thrust and torque coefficients and efficiency values versus inclination angle.

δ (º)	0	5	10
K_T	0.1672	0.1603	0.1586
$10K_Q$	0.2961	0.2826	0.2801
η (%)	71.9	72.2	72.1

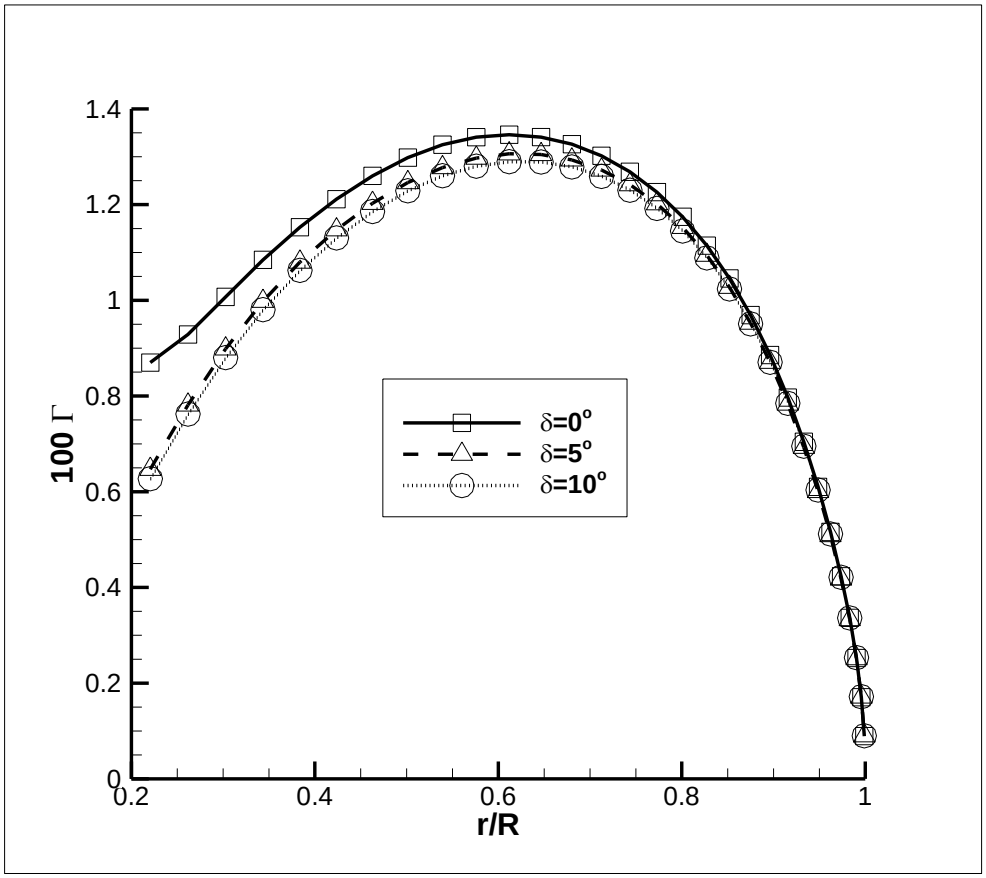

Figure 8. Average circulation (loading) distribution on blades versus inclination shaft angle.

Later, the pitch ratios (P/D) of the model propeller have been increased in five percent (5%) rate as given in Table 3, while all other geometric factors have been kept fixed. Advance coefficient is also same as in previous case, J = 0.8 and the cavitation number is selected as σ = 1.2. The computed cavitation patterns on blades for different shaft inclination angles (δ = 0º, 5º and 10º) are shown in Figures 9, 10 and 11, respectively. As it is clear from these figures that an increase in inclination angle causes a decrease in cavitation lengths on the blade of the top side while an increase on the blade of the bottom side. This result is similar to the previous case with original pitch ratios. Note also that the loading (increased cavity volume) on the blades has been increased due to the increase in pitch ratios.

Table 3. New pitch ratios.

r/R	0.2	0.3	0.4	0.5	0.6	0.7	0.8	0.9	0.95	0.98	1.0
P/D	1.1603	1.1587	1.1573	1.1532	1.1479	1.1423	1.1381	1.1352	1.1324	1.1309	1.1288

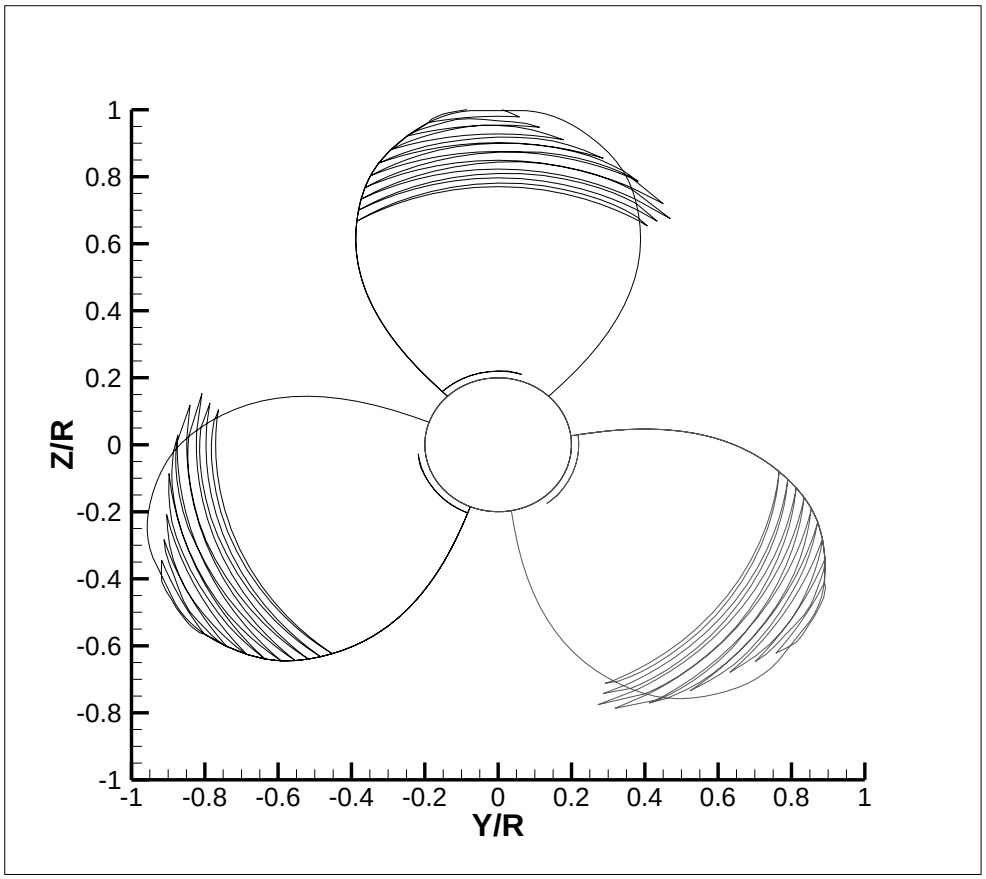

Figure 9. Cavitation pattern on blades for J=0.8, σ=1.2 and δ=0º with new pitch ratios.

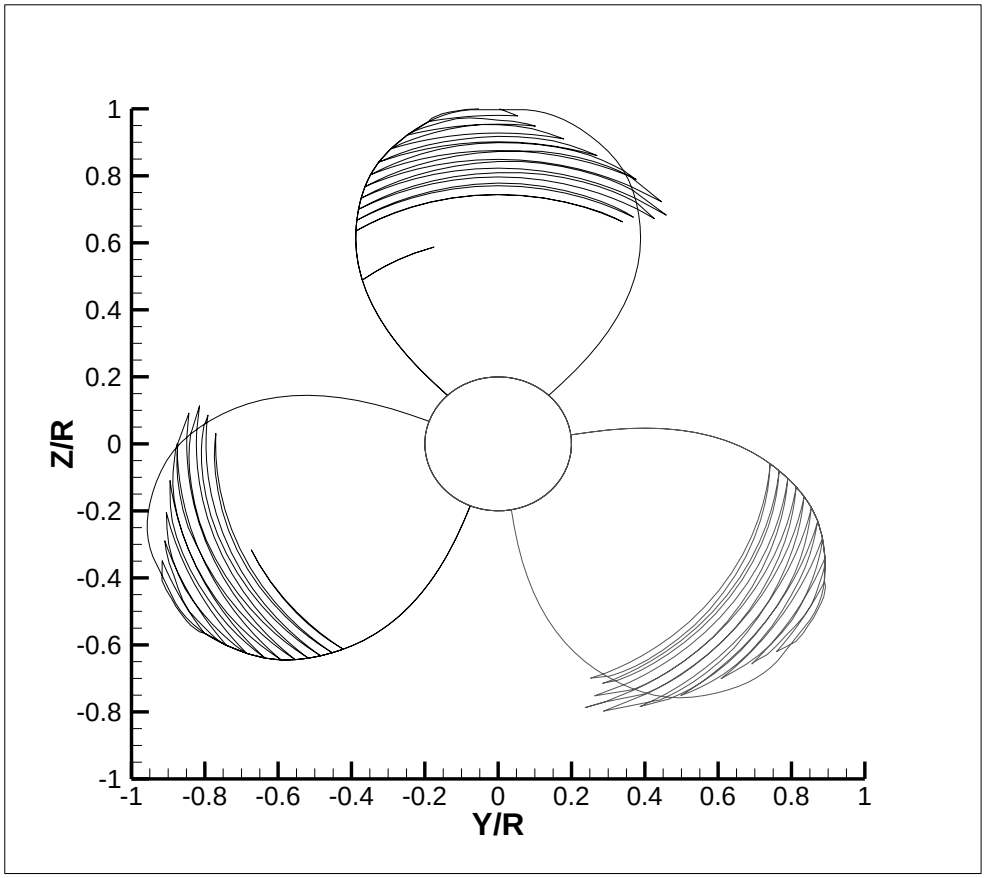

Figure 10. Cavitation pattern on blades for J=0.8, σ=1.2 and δ=5º with new pitch ratios.

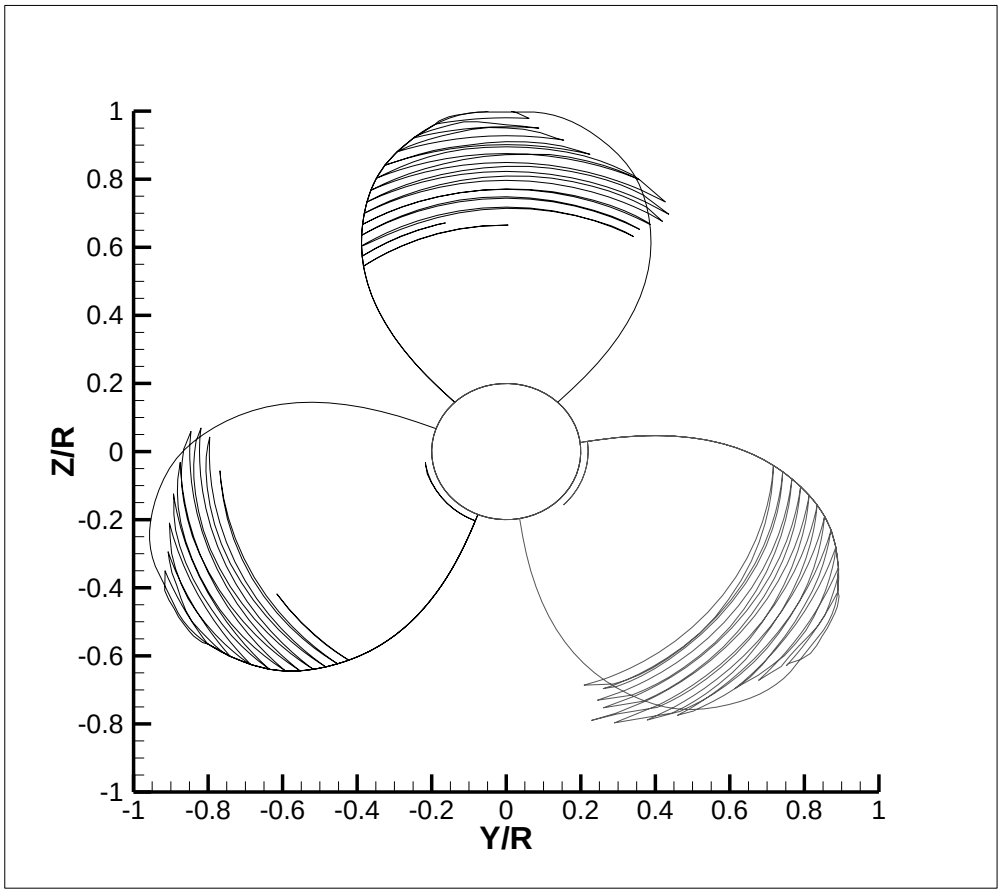

Figure 11. Cavitation pattern on blades for J=0.8, σ=1.2 and δ=10º with new pitch ratios.

4. CONCLUSION

In this study the inclination angle effects on cavitating propellers under open water conditions have been investigated by a numerical lifting surface method. The DTMB 4119 propeller has been chosen for validation of the numerical method. The findings can be summarized as follows:

1-) An increase in inclination angle is causing a decrease in loading (thrust and torque coefficients) on the blades of propeller under cavitating condition.

2-) An increase in inclination angle is causing no change in efficiency of the propeller under cavitating condition. It can be said that the inclination angle can be applied up to a certain value if the thrust coefficient generates the required actual thrust value.

3-) An increase in inclination angle of shaft is causing a decrease in cavity length and volume on the sections when the blade is on the top (upper) side of rotating plane while it causes an increase when the blade is on the bottom (lower) side of the rotating plane.

NOMENCLATURE

a	NACA camber (mean) line constant
c(r)	Chord length along blade (m)
D	Propeller diameter (m)
f_{max}	Maximum camber of each blade section (m)
J	Advance coefficient =U/(nD)
NB	Number of blades
K_T	Thrust coefficient of propeller =$T/(\rho n^2 D^4)$
K_Q	Torque coefficient of propeller =$Q/(\rho n^2 D^5)$
n	Propeller rotational speed [rps]
$\vec{n}_m$	Unit vector normal to the mean camber or trailing wake surface
P(r)	Pitch of blade section (m)

Q	Propeller torque (Nm)
Q_B	Blade source strength (m^3/sec)
Q_C	Cavity source strength (m^3/sec)
r	Radial parameter (m)
r_h	Radius of hub (m)
R	Radius of propeller (m)
t	Thickness parameter for blade sections (m)
t_{max}	Maximum thickness of each blade section (m)
T	Propeller thrust (N)
U	Uniform incoming flow velocity (m/sec)
$\vec{v}_\Gamma$	Velocity vector induced by each unit strength vortex element (m/sec)
$\vec{v}_Q$	Velocity vector induced by each unit strength source element (m/sec)
δ	Inclination angle of shaft (degree)
$\beta(r)$	Pitch angle of blade section (degree)
η	Propeller efficiency $=J/(2\pi)K_T/K_Q$
Γ	Circulation
ω	Angular velocity $=2\pi$ n (rad/sec)
ρ	Density of water (kg/m^3)

REFERENCES

[1] Kerwin J. E., Lee C. S., "Prediction of steady and unsteady marine propeller performance by numerical lifting surface theory", Transactions SNAME 1978.

[2] Kuiper G., Jessup S. D., "A propeller design method for unsteady conditions", Transactions SNAME 1993, 101, 247-273.

[3] Kerwin, J. E., Keenan, D. P., Black, S. D., Diggs, J.D., "A coupled viscous/potential flow design method for wake-adapted, multi-stage, ducted propulsors using generalized geometry", Transactions SNAME 1994**,** 102, 23-56.

[4] Griffin, P. E., Kinnas, S. A., "A design method for high-speed propulsor blades", Journal of Fluids Engineering 1998**,** 120, 556–562.

[5] Bal, S., Guner, M., "Performance analysis of podded propulsors", Ocean Engineering 2009, 36, 556-563.

[6] Gaggero, S., Villa, D., Brizzolara, S., "RANS and panel method for unsteady flow propeller analysis", Journal of Hydrodynamics 2010, 22, 5, 564-569.

[7] Krasilnikov, V. I., Zhang, Z., Hong, F., "Analysis of unsteady blade forces by RANS", First International Symposium on Marine Propulsors, Trondheim, Norway, 2009.

[8] Tani, G., Viviani, M., Villa, D., Ferrando, M., "A study on the influence of hull wake on model scale cavitation and noise tests for a fast twin screw vessel with inclined shaft", Proceedings of the Institution of Mechanical Engineers, Part M, Journal of Engineering for the Maritime Environment 2018, 232, 307-330.

[9] Renick, D. H., "Unsteady propeller hydrodynamics", PhD thesis, MIT, USA, 2001.

[10] Brizzolara, S., Villa, D., Gaggero, S., "A Systematic comparison between RANS and panel methods for propeller analysis", Proc. of 8th International Conference on Hydrodynamics, Nantes, France, Sep. 30-Oct. 3, 2008.

[11] Kerwin, J. E., Hadler, J. B., Principles of Naval Architecture Series: Propulsion, The Society of Naval Architects and Marine Engineers (SNAME), USA, 2010.

[12] Greely, D. S., Kerwin, J. E., "Numerical methods for propeller design and analysis in steady flow", Transactions SNAME 1982, 90, 415-453.

[13] Kinnas, S.A., Griffin, P., Choi, J-K., Kosal, E. M., "Automated design of propulsor blades for high-speed ocean vehicle applications", Transactions SNAME 1998, 106.

[14] Szantyr, J.A. "A Method for analysis of cavitating marine propellers in non-uniform flow", International Shipbuilding Progress 1994, 41, 223-242.

[15] Celik, F., Guner, M., "Improved lifting line method for marine propeller", Marine Technology 2006, 43, 100-113.

[16] Yilmaz, N., Khorasanchi, M., Atlar, M., "An investigation into computational modelling of cavitation in a propeller's slipstream", 5th International Symposium on Marine Propulsion, Espoo, Finland, 2017.

[17] Kinnas, S. A., Pyo, S., "Cavitating propeller analysis including the effects of wake alignment", Journal of Ship Research 1999, 43, 38-47.

[18] Bal, S., "A practical technique for improvement of open water propeller performance", Proceedings of the Institution of Mechanical Engineers, Part M, Journal of Engineering for the Maritime Environment 2011, 225, 375-386.

[19] Bal, S., "A method for optimum cavitating ship propellers", Turkish Journal of Engineering and Environmental Sciences 2011, 35, 139-158.

[20] Carlton, J.S. Marine propellers and propulsion, Oxford: Elsevier (Butterworth-Heinmann) Publ, 2012.